Supporting Information

Proximity-induced FRET and charge transfer between quantum dots and curcumin enable reversible thermochromic hybrid polymeric films

Jefin Parukoor Thomas,[ac] R. B. Amal Raj,[a] G. Virat,[ac] Amarjith V. Dev,[bc] Chakkooth Vijayakumar[bc] and E. Bhoje Gowd[*ac]

[a]Materials Science and Technology Division
CSIR-National Institute for Interdisciplinary Science and Technology, Trivandrum 695 019, Kerala, India.
[b]Chemical Sciences and Technology Division
CSIR-National Institute for Interdisciplinary Science and Technology, Trivandrum 695 019, Kerala, India.
[c]Academy of Scientific and Innovative Research (AcSIR), Ghaziabad 201 002, India.

* Author for correspondence: E-mail: bhojegowd@niist.res.in

Table of contents

EXPERIMENTAL SECTION

Poly[(R)-3-hydroxybutyric acid] (PHB) of M_n ~ 241,000 and $Đ$~ 2.62 obtained commercially in white powdered form supplied by Sigma Aldrich, *h*-BN powder having lateral sizes ~1 μm, curcumin powder, polyethylene glycol (PEG) (M_w ~6000), *N, N*-dimethylformamide (DMF) and chloroform were procured from Sigma-Aldrich.

Synthesis of Boron Nitride Quantum Dots (QDs)

Boron nitride quantum dots were synthesized based on literature procedures with slight modifications.[1] Initially, boron nitride nanosheets (BNNSs) dispersion was prepared by dispersing *h*-BN powder in DMF in a 250 mL beaker and sonicated using an ultrasonicator for 6 h. Then, the BNNSs dispersion was transferred into a Teflon-lined stainless steel autoclave and solvothermally treated at 200 °C for 24 h in a vacuum oven. Later, it was allowed to cool down to room temperature naturally and the resulting suspensions were centrifuged at 8000 rpm for 15 min to remove the precipitated BNNSs. The supernatant solution was filtered through a 0.22 μm microporous membrane and a slight yellow-colored solution of BNQDs was collected.

Synthesis of PEG-modified Boron Nitride Quantum Dots (PQDs)

For the modification of BNQDs, 0.3 g of PEG 6000 was mixed with the BNNSs dispersion (prepared as discussed above). It was thoroughly mixed using an ultrasonicator. Then, the mixture was transferred into a Teflon-lined stainless steel autoclave and solvothermally treated at 200 °C for 24 h in a vacuum oven. The mixture was allowed to cool down to room temperature and the resulting solution was filtered as mentioned above and the prepared PEG modified BNQDs were designated as PQDs.

Synthesis of PHB/ Curcumin film (PHB/Cur)

The PHB/Curcumin film was prepared through the solution casting method. Curcumin (1 wt%) dissolved in chloroform was added to a homogenous solution of PHB in chloroform and stirred

thoroughly. The resulting solution was used to cast the film, which was then dried in a vacuum oven at 40 °C overnight to remove residual solvents. The sample was designated as PHB/Cur.

Synthesis of PHB/Cur-PQDs Hybrid film (PHB/Cur-PQDs)

For the preparation of hybrid films, different volumes (5 and 10 mL) of PQDs solution in DMF were added to a homogenous PHB/Cur solution in chloroform (prepared as mentioned above). The resulting hybrid solution was stirred continuously for 12 h and then was kept for solvent evaporation to obtain the film. The obtained as-cast films were dried at 40 °C in a vacuum oven for 24 h. The weight percent of PQDs was estimated to be 6 wt% and 12 wt% for 5 mL and 10 mL of PQDs solution, respectively.

Synthesis of PHB/Cur-QDs Hybrid film (PHB/Cur-QDs)

The hybrid PHB/Cur-QDs film was prepared using unmodified QDs by the same procedure adopted for the fabrication of PHB/Cur-PQDs film as mentioned above and the prepared hybrid film was designated as PHB/Cur-QDs.

CHARACTERIZATION

To examine the morphology of QDs and PQDs, a JEOL 2010 multipurpose high-resolution transmission electron microscope (TEM) operating at 300 kV was used. The dispersed QDs solution was drop cast on a carbon-coated copper grid and was dried under a vacuum before the analysis. Infrared spectra were recorded using PerkinElmer Series FT-IR spectrum-2 over the wavenumber range of 4000−400 cm^{-1}. The FTIR/ATR spectra were collected at atmospheric conditions with a resolution of 4 cm^{-1} and 32 scans. The UV/Visible absorption spectra measurements were done at room temperature on the SHIMADZU UV-2600 spectrophotometer. Photoluminescence spectra were measured via the SPEX-Flourolog-3 (Horiba) spectrofluorimeter equipped with a 450 W Xenon flash lamp source. The fluorescence lifetime decay curves were obtained by the time-correlated single photon counting (TCSPC) technique (Horiba, DeltaFlex) employing 331 nm as an excitation source and Picosecond

photon detection module (PPD-850) as a detector. The fluorescence lifetime values were estimated using DAS6 decay analysis software by deconvoluting the instrument response function with tri-exponential decay. The decay of the fluorescence intensity (I) was fitted with a tri-exponential function.

$$I = A_1 e^{-t/\tau_1} + A_2 e^{-t/\tau_2} + A_3 e^{-t/\tau_3}$$

Where τ_1, τ_2, and τ_3 correspond to the decay lifetimes of the luminescence, and A_1, A_2, and A_3 are their respective amplitudes.

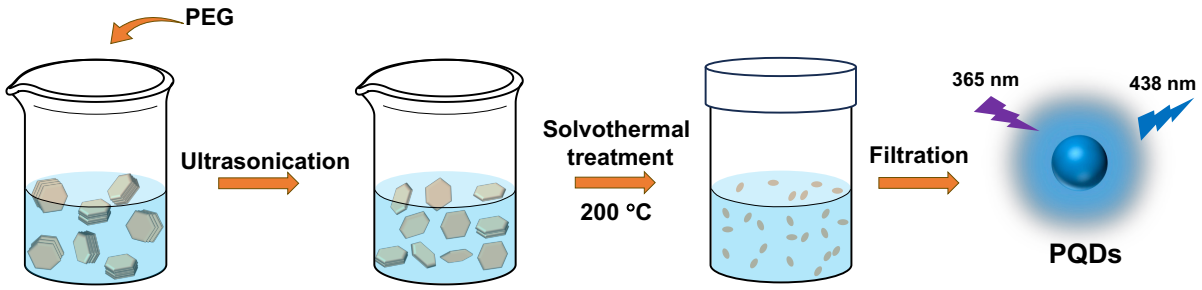

Figure S1. Synthetic procedure for the PQDs through solvothermal treatment.

QDs were prepared through a solvothermal route using exfoliated boron nitride nanosheets in DMF at 200 °C for 24 h. TEM images depicted that the lateral dimension ranged from 1.5 to 4 nm with slight aggregation of quantum dots as shown in Fig. S2a & b. QDs exhibited blue color emission under UV light. It was noticed that the fluorescence intensity was reduced due to a slight aggregation of quantum dots at room temperature. To improve the stability of QDs, surface passivation was done by introducing PEG. Fig. S1 depicts the synthesis method for the preparation of PQDs. The resulting PQDs were uniformly distributed as revealed from TEM images which show an average lateral size of ~ 3.5 nm as shown in Fig. S2c & d. In addition, we can observe that the PEG chains are adsorbed on the surface of QDs. The presence of PEG chains on the surface of the QDs improves the fluorescence intensity due to the uniform dispersion and stabilization of PQDs.

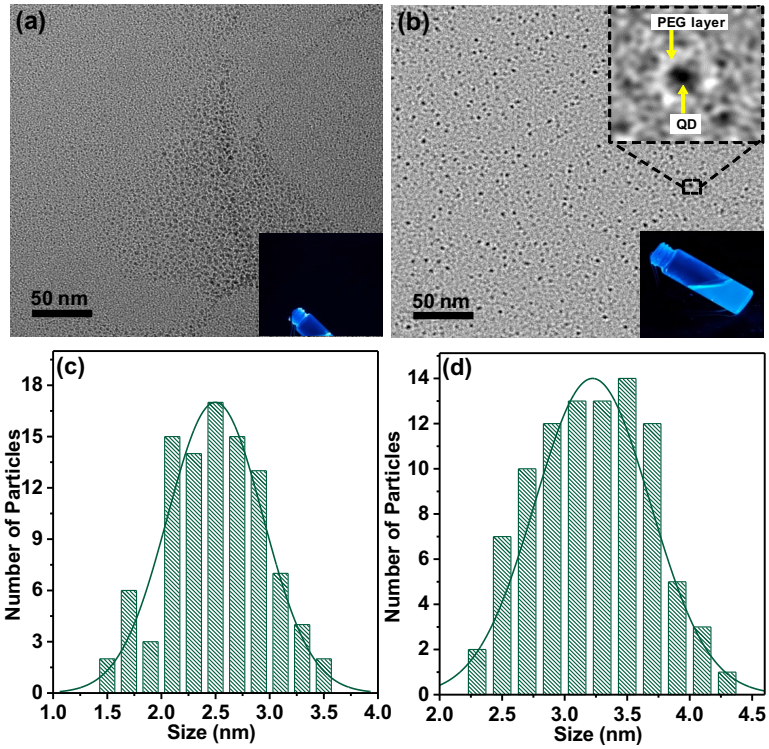

Figure S2. TEM images of (a) QDs, (b) PQDs (Inset: a magnified image of a PQD showing the PEG aggregation on the surface of QD) and the size distribution histograms of (c) QDs and (d) PQDs.

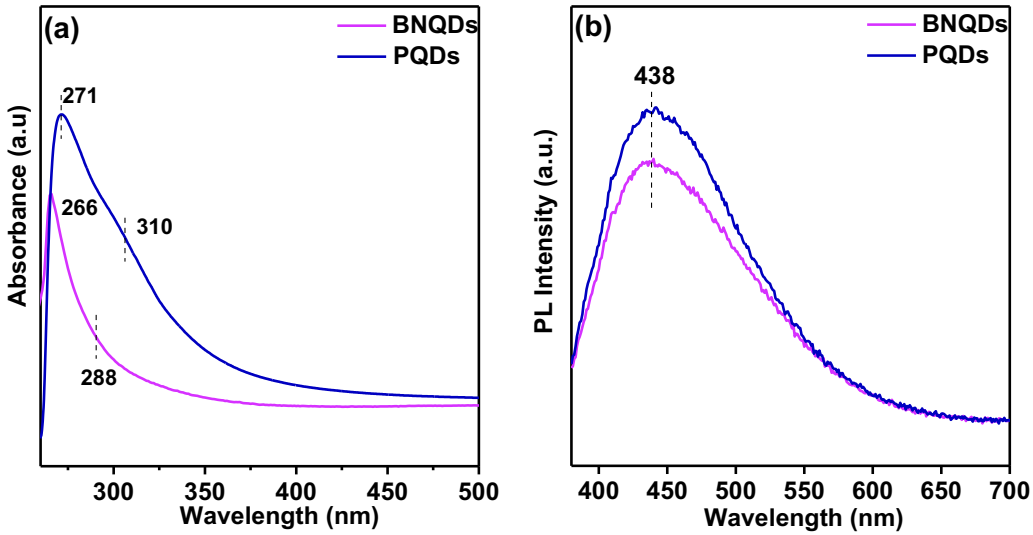

Figure S3. (a) UV-visible absorption spectra and (b) PL emission spectra of QDs and PQDs.

The UV-visible absorption spectra displayed in Fig. S3a show typical absorption bands of QDs at 266 nm and a shoulder band at around 288 nm.[1, 2] In PQDs, a red shifting was observed to 271 nm and shoulder band to 310 nm as PEG acts as surface passivating agents on

the surface of QDs. From the PL spectra given in Fig. S3b, PL emission maxima for both QDs and PQDs are observed at 438 nm. The fluorescence intensity of PQDs appeared to be higher compared to that of QDs due to the surface passivation effect of PEG.

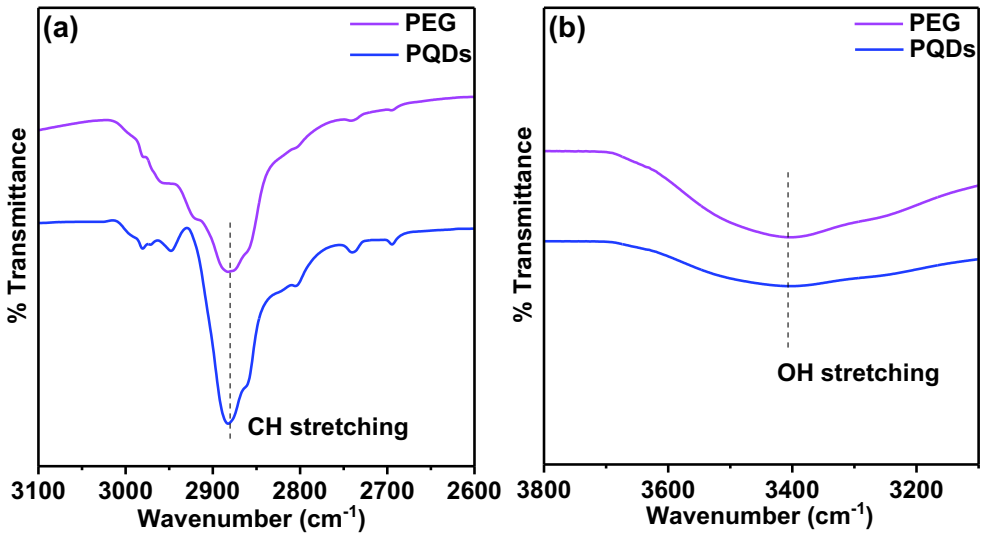

Figure S4. FTIR spectra of PEG and PQDs in the region of (a) 3100-2600 cm^{-1} and (b) 3800-3100 cm^{-1}.

In the FTIR spectra of PQDs and PEG, the major IR peaks of PEG are also observed in PQDs with trivial shifts in the position of peaks indicating the surface passivation of QDs using PEG.

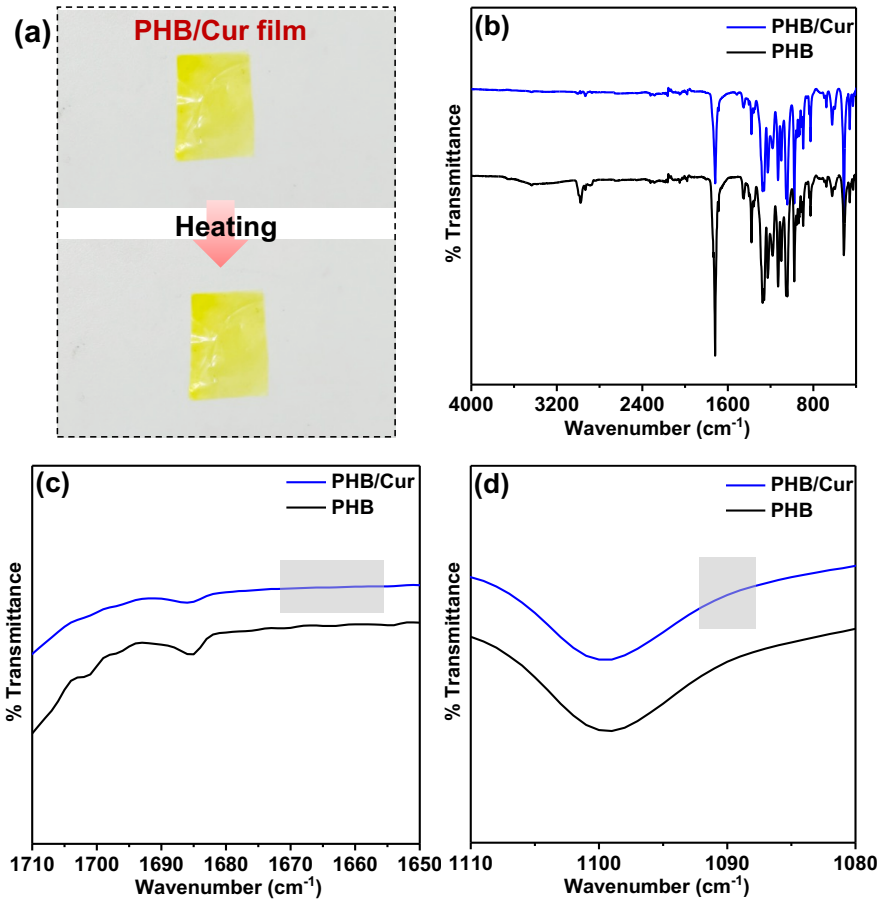

Figure S5. (a) Photograph of PHB/Cur film prepared in DMF solvent before and after heating. (b) FTIR spectra of PHB/Cur and PHB full spectra and in the regions (c) 1710-1650 cm^{-1} and (d)1110-1080 cm^{-1} depicting the absence of DMF-Cur interactions.

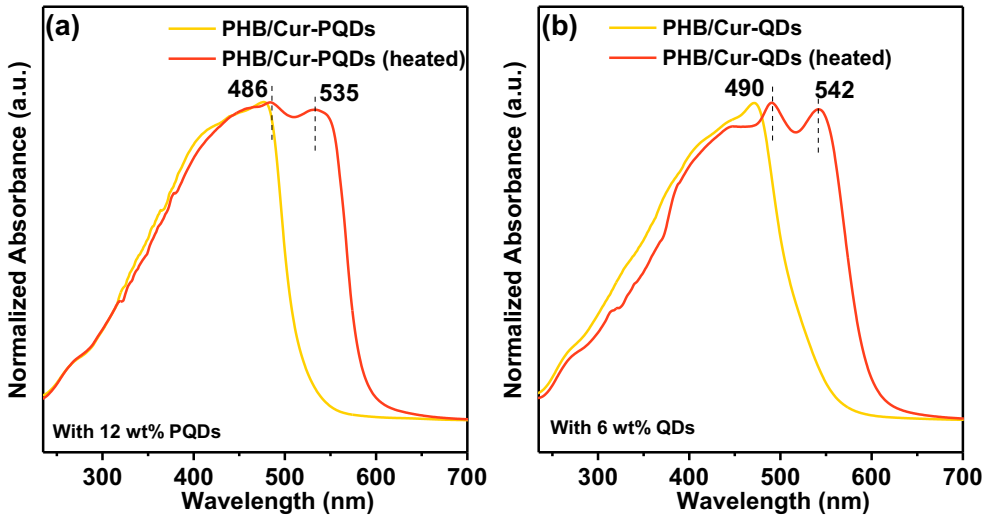

Figure S6. UV-visible absorption spectra of (a) PHB/Cur-PQDs (with 12 wt% PQDs), and (b) PHB/Cur-QDs (with 6 wt% QDs) before and after heating.

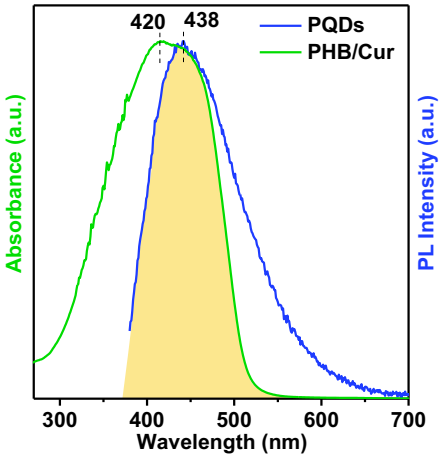

Figure S7. Spectral overlap of absorption of PHB/Cur with emission band of PQDs.

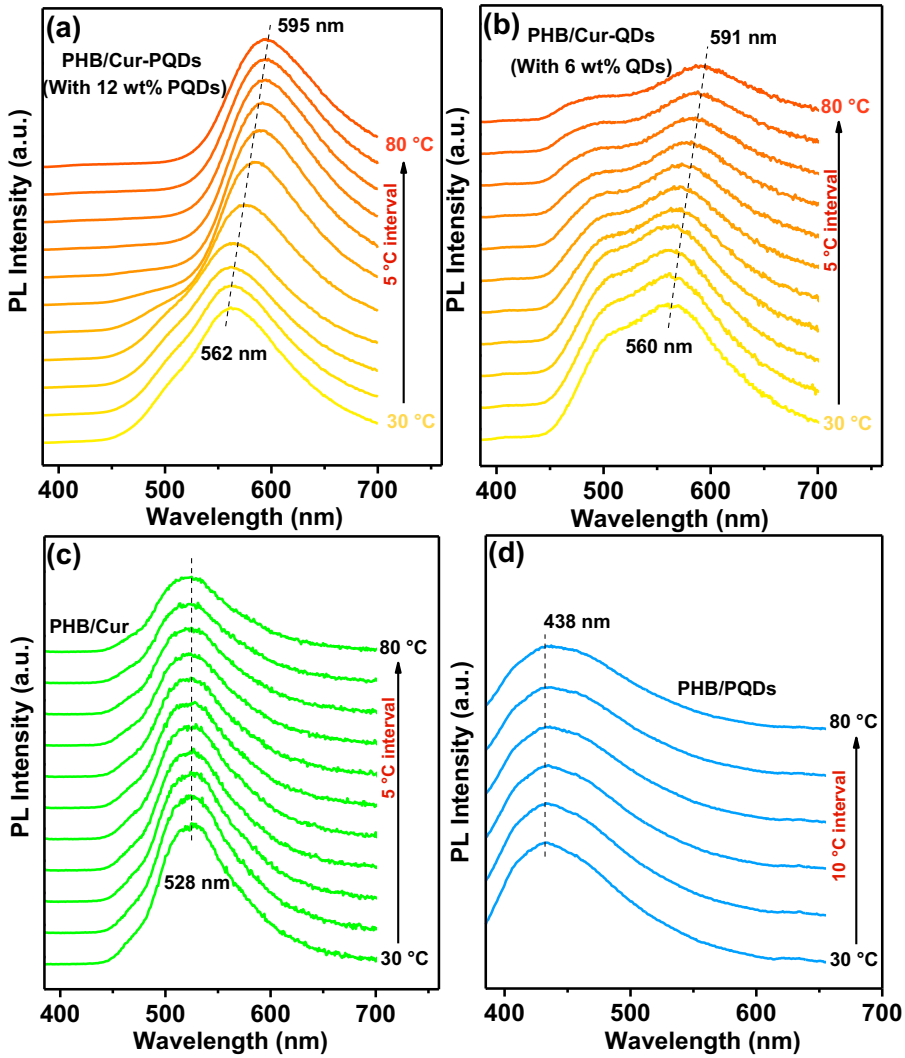

Figure S8. Temperature-dependent PL spectra of (a) PHB/Cur-PQDs (with 12 wt% of PQDs), (b) PHB/Cur-QDs (with 6 wt% of QDs), and (c) PHB/Cur and (d) PHB/PQDs (with 6 wt% of PQDs) recorded from room temperature to 80 °C.

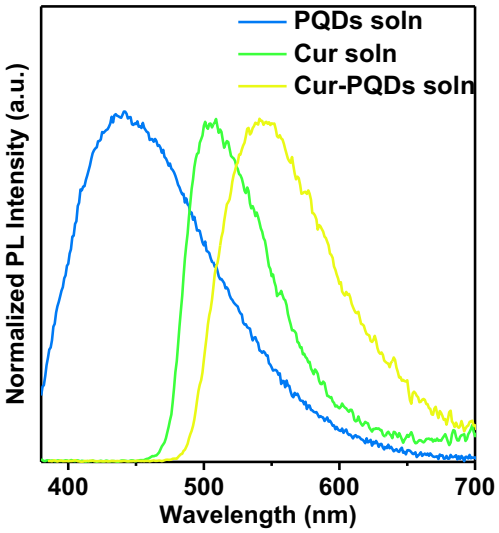

Figure S9. PL Emission spectra of PQDs, Cur, and Cur-PQDs blend in solution state.

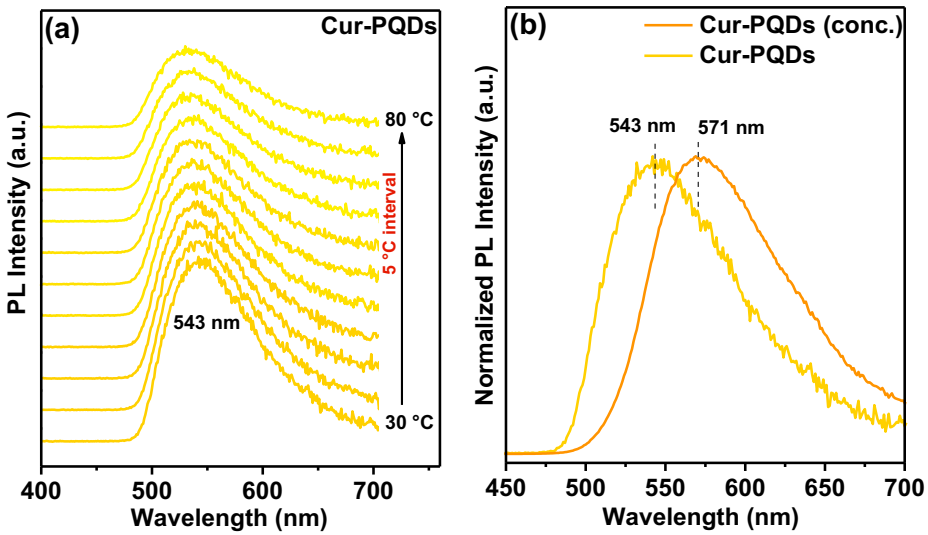

Figure S10. (a) Temperature-dependent PL spectra of Cur-PQDs and (b) PL emission spectra of Cur-PQDs (conc.) and Cur-PQDs dilute solution.

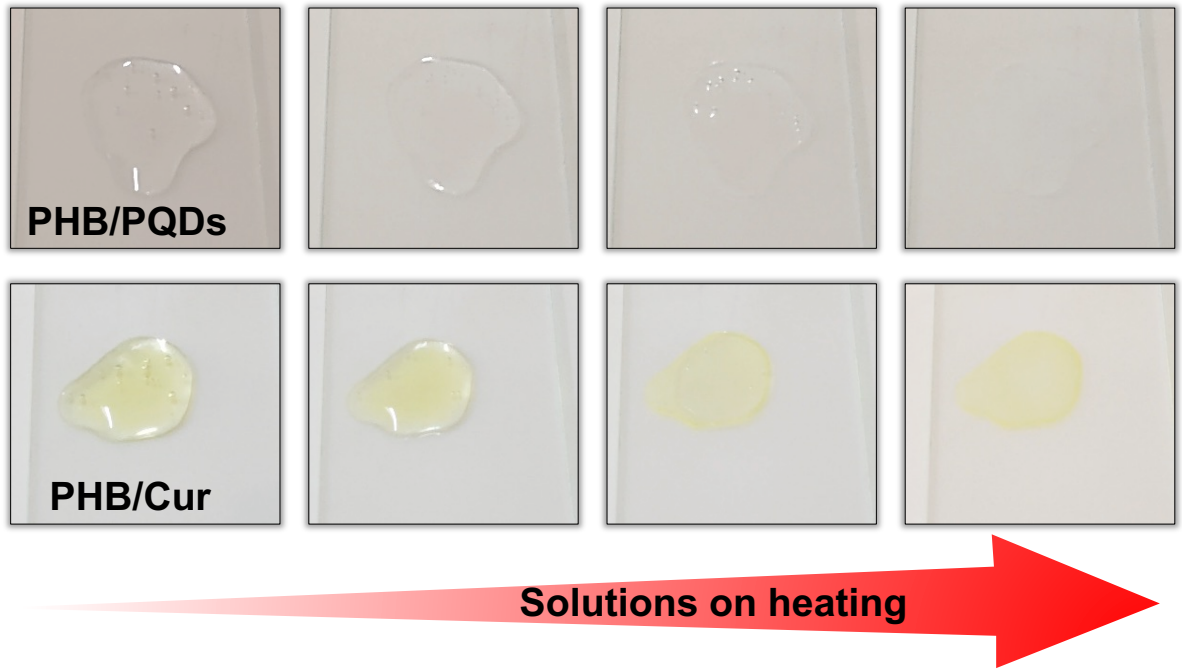

Figure S11. Photographs displaying PHB/PQDs and PHB/Cur solutions upon heating.

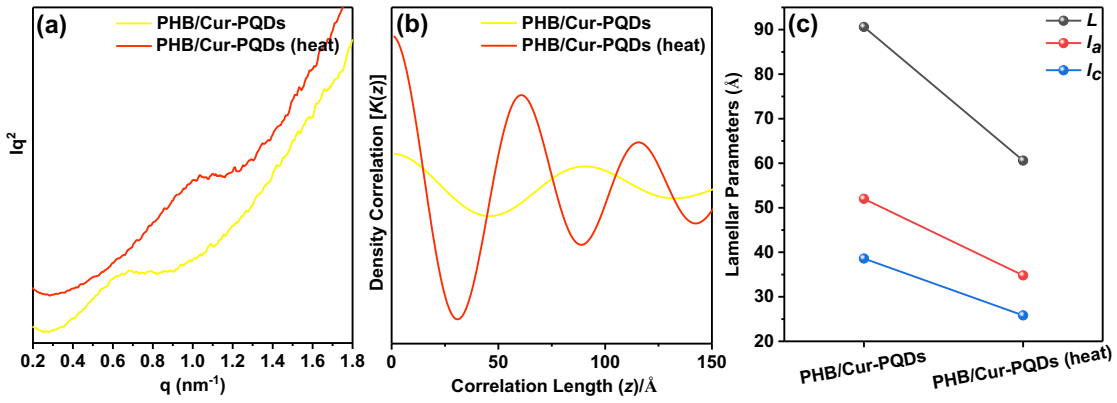

Figure S12. (a) Small-angle X-ray scattering patterns, (b) corresponding one-dimensional correlation function curves, and (c) lamellar parameters (long period (L), crystalline lamellar thickness (l_c) and amorphous layer thickness (l_a)) estimated as described in our previous article[3] from (b) for PHB/Cur-PQDs before and after heating.

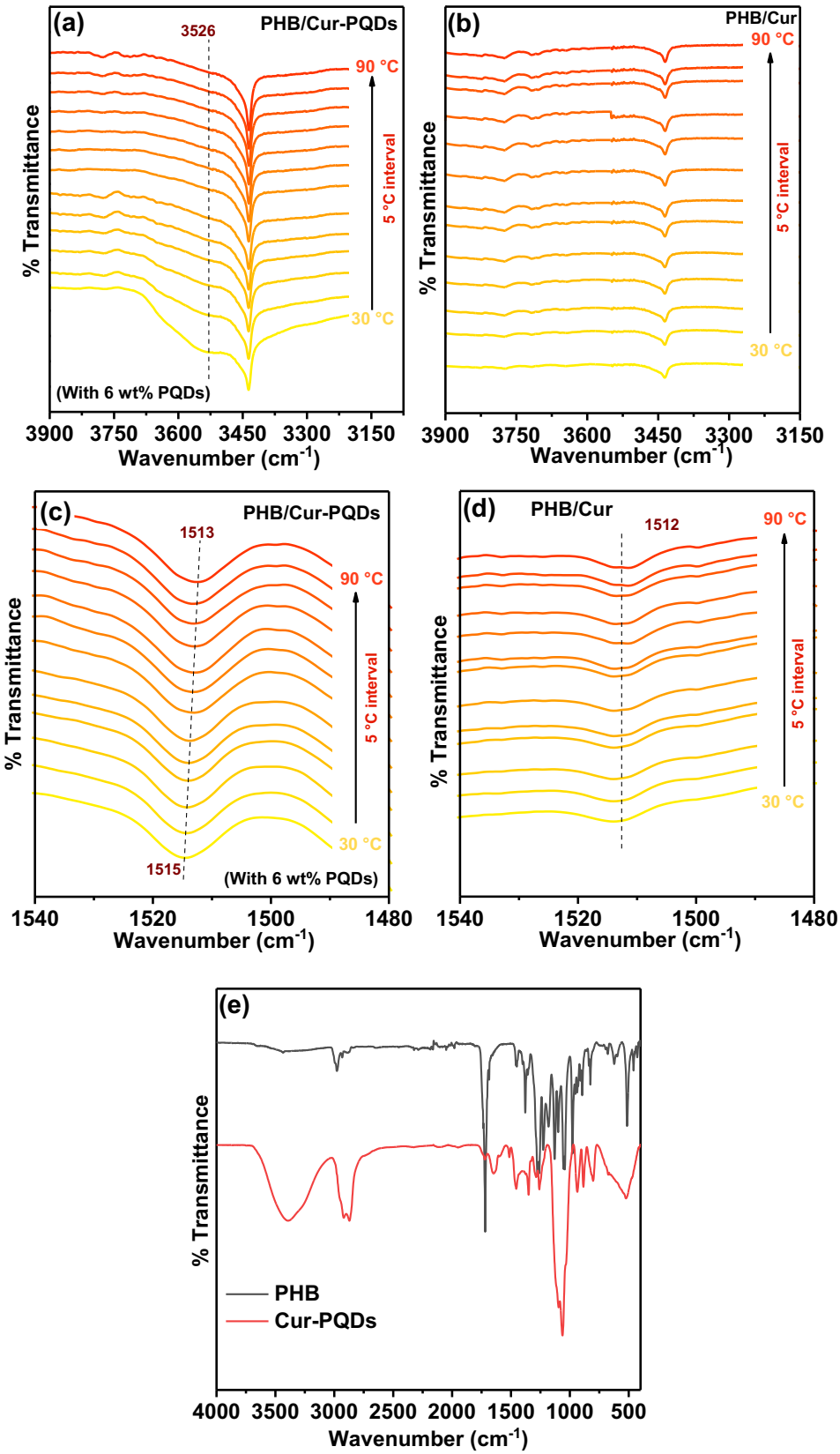

Figure S13. FTIR spectra of PHB/Cur-PQDs (with 6 wt% PQDs) and PHB/Cur in the regions (a & b) 3900 - 3075 cm^{-1} and (c & d) 1540 - 1480 cm^{-1}. (e) FTIR spectra of PHB and Cur-PQDs.

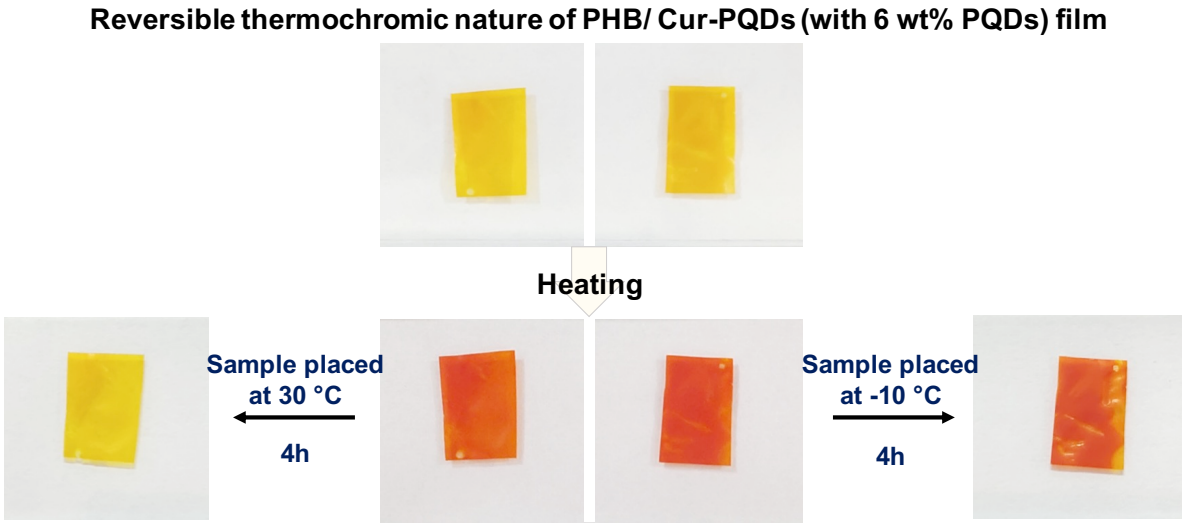

Figure S14. Photographs of PHB/Cur-PQDs films (with 6 wt% PQDs) at room temperature, after heating, and after 4h (placing the heated samples at 30 °C and -10 °C).

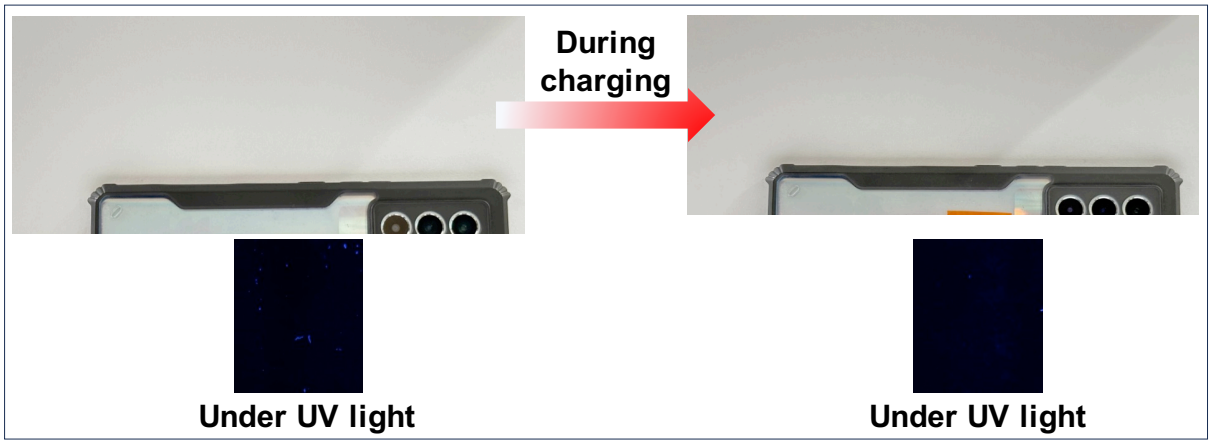

Figure S15. Photographs of PHB/Cur-PQDs films as a temperature sensor for mobile phones to detect overheating during charging.

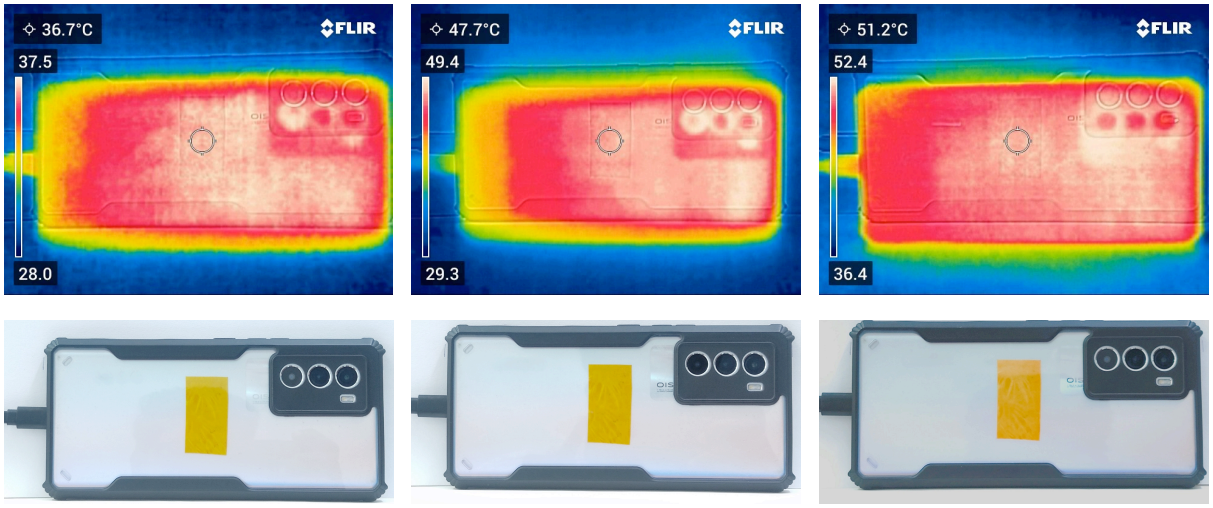

Figure S16. IR images and photographs of PHB/Cur-PQDs films exhibiting the gradual colour change with temperature.

Table S1. Time-resolved fluorescence decay parameters of PHB/PQDs, PHB/Cur-PQDs, and PHB/Cur-PQDs (heat) with 6 wt% of PQDs.

Sample	τ_1 (intrinsic state) (ns)	τ_2 (defect state) (ns)	τ_3 (aggregate state) (ns)	$<\tau>$ (ns)	χ^2
PHB/PQD	3.5 (40.61%)	12.2 (31.93%)	0.4 (27.47%)	1.27	1.19
PHB/Cur-PQD	5.5 (0.54%)	374.4 (7.03%)	0.06 (92.43%)	0.07	1.16
PHB/Cur-PQD (heat)	9.8 (1.54%)	253.6 (13.02%)	0.15 (85.44%)	0.17	1.19

References

1. H. Li, R. Y. Tay, S. H. Tsang, X. Zhen and E. H. T. Teo, *Small*, 2015, **11**, 6491-6499.
2. L. Chen, X. Zhang, Z. Zhao, F. Wang, Y. Huang, C. Bai, L. An and Y. Yu, *Colloids and Surfaces A: Physicochemical and Engineering Aspects*, 2021, **614**, 126181.
3. P. Shaiju, N. S. Murthy and E. B. Gowd, *Macromolecules*, 2016, **49**, 224-233.